European Journal of Nuclear Medicine and Molecular Imaging (2019) 46:677–685
https://doi.org/10.1007/s00259-018-4193-y

ORIGINAL ARTICLE

Biodistribution and radiation dose estimates for ^{68}Ga-DOTA-JR11 in patients with metastatic neuroendocrine tumors

Simone Krebs[1] · Neeta Pandit-Taskar[1,2] · Diane Reidy[2,3] · Bradley J. Beattie[4] · Serge K. Lyashchenko[1,2,5] · Jason S. Lewis[1,2,5] · Lisa Bodei[1,2] · Wolfgang A. Weber[1,2,6] · Joseph A. O'Donoghue[4]

Received: 17 April 2018 / Accepted: 10 October 2018 / Published online: 29 October 2018

Abstract

Purpose Somatostatin receptor antagonists have shown promise for imaging neuroendocrine tumors (NETs) in preclinical studies, but clinical data is still very limited. In this study, we assess the feasibility of using the novel somatostatin antagonist ^{68}Ga-DOTA-JR11 for PET imaging of NETs.

Methods Twenty patients with advanced NETs underwent whole-body PET/CT imaging 60 min after injection of 169 MBq (median) ^{68}Ga-DOTA-JR11 as part of a prospective study. Volumes of interest were drawn around up to four ^{68}Ga-DOTA-JR11-avid lesions per patient (with uptake greater than liver) and standardized uptake values were estimated. Additionally, target-to-normal tissue ratios were calculated. A subset of six patients had additional imaging (25-min dynamic scan of the upper abdomen including, at least partly, cardiac left ventricle, liver, spleen, and kidney, and a whole-body PET/CT scan at 30 min post-injection) to determine the time course of tracer distribution and facilitate radiation dose estimates. Absorbed doses were calculated using OLINDA/EXM 1.0.

Results In contrast to the known biodistribution of somatostatin receptor agonists, little or no uptake above background was seen in the pituitary gland, spleen, adrenals, and uninvolved liver; e.g., median spleen SUV_{mean} 1.4 (range: 0.7–1.8), liver SUV_{mean} 1.1 (0.7–1.9). A total of 42 tumor lesions were analyzed with median SUV_{max} 13.0 (range: 2.9–94), TNR blood 9.3 (1.8–87), TNR spleen 4.9 (1.9–48), TNR kidney 2.2 (0.52–28), and TNR liver 10.5 (2.3–107). Tumor uptake reached plateau levels by 20-30 min post-injection. The highest absorbed dose estimates (mGy/MBq) to normal tissues were: urinary bladder wall (0.30; SD 0.06) and kidneys (0.050; SD 0.013). The effective dose (ICRP 103) was 0.022 (SD 0.003) mSv/MBq.

Conclusions ^{68}Ga-DOTA-JR11 demonstrated rapid tumor uptake, high tumor/background ratios, and rapid clearance from blood. The low liver background is advantageous and may facilitate detection of liver metastases. Dosimetric data compare favorably with published data for ^{68}Ga-DOTATATE and ^{68}Ga-DOTATOC.

Keywords Somatostatin receptor antagonists · JR11 · PET/CT · Neuroendocrine tumors

Electronic supplementary material The online version of this article (https://doi.org/10.1007/s00259-018-4193-y) contains supplementary material, which is available to authorized users.

✉ Simone Krebs
krebss@mskcc.org

[1] Department of Radiology, Memorial Sloan Kettering Cancer Center, 1275 York Avenue, New York, NY 10065, USA

[2] Department of Radiology, Weill Cornell Medical College, New York, NY, USA

[3] Department of Medicine, Memorial Sloan Kettering Cancer Center, New York, NY, USA

[4] Department of Medical Physics, Memorial Sloan Kettering Cancer Center, New York, NY, USA

[5] Radiochemistry and Molecular Imaging Probes Core, Memorial Sloan Kettering Cancer Center, New York, NY, USA

[6] Department of Nuclear Medicine, Technical University of Munich, Munich, Germany

Introduction

Neuroendocrine tumors (NETs) represent a heterogenous group of tumors with significantly increasing incidence. For example, gastroenteropancreatic neuroendocrine tumors (GEP-NETs), the largest subgroup of NETs, underwent a striking increase in incidence from 1.0/100,000 in 1973 to 3.65/100,000 in the period 2003–2007 [1] in the US.

Overexpression of somatostatin receptors and specifically the somatostatin receptor subtype 2 (SSTR2) is a common feature of NETs. Radiolabeled, metabolically stable somatostatin receptor-binding peptides have been used clinically for imaging of NETs since 1994 [2]. The first FDA-approved agent was ^{111}In-octreotide (Octreoscan®). More recently, several ^{68}Ga-labeled somatostatin analogues enabling SSTR positron emission tomography/computed tomography (PET/CT) with improved binding affinity and biodistribution have been introduced. One of these agents, ^{68}Ga-DOTA-TATE, was FDA-approved in 2016 [3]. All of these imaging agents are somatostatin agonists; i.e., they stimulate the somatostatin receptor and are consequently internalized.

Preclinical studies have indicated that SSTR antagonists bind to significantly more receptor sites than the agonists currently used for peptide receptor radionuclide therapy (PRRT) [4]. This finding was confirmed by quantitative autoradiography of patient-derived tumor samples [5], demonstrating a more than four-fold increase in the ex-vivo binding of the somatostatin receptor antagonist ^{177}Lu-DOTA-BASS compared to the agonist ^{177}Lu-DOTA-TATE. Wild et al. performed a preliminary clinical study comparing the dosimetry of a ^{177}Lu-labeled therapeutic SSTR antagonist ^{177}Lu-DOTA-JR11 with ^{177}Lu-DOTA-TATE in four patients. In this study, the antagonist demonstrated, on average, a three-fold higher tumor dose and a two-fold higher tumor-to-kidney ratio [6]. PET and biodistribution studies in mice bearing SSTR2-expressing xenografts also demonstrated higher tumor uptake of ^{68}Ga-DOTA-JR11 and ^{68}Ga-NODAGA-JR11 (^{68}Ga-OPS202) than the high-affinity SSTR2 *agonist* ^{68}Ga-DOTA-TATE [7], supporting further clinical evaluation of these imaging agents.

Nicolas et al. recently reported two clinical studies [8, 9] on the use of ^{68}Ga-NODAGA-JR11 (^{68}Ga-OPS202) to image GEP-NETs. The first of these studies [8] focused on biodistribution, safety, and radiation dosimetry, while the second directly compared the biodistribution of ^{68}Ga-NODAGA-JR11 (^{68}Ga-OPS202) with that of the SSTR2 agonist ^{68}Ga-DOTA-TOC, and found the antagonist to be superior in terms of lesion contrast, detection, and sensitivity [9].

The purpose of this study was to assess the utility of the novel somatostatin antagonist ^{68}Ga-DOTA-JR11 for PET imaging of NETs. Patients with advanced NETs and positive ^{111}In-pentetreotide (OctreoScan®) scans were imaged with ^{68}Ga-DOTA-JR11 prior to PRRT with ^{177}Lu-DOTA-JR11. Detailed biodistribution and radiation dosimetry was investigated on a subset of these patients.

Materials and methods

Clinical study with ^{68}Ga-DOTA-JR11

Under the auspices of a protocol approved by the Institutional Review Board and an Investigational New Drug application approved by the FDA, 20 patients (ten male, ten females, age: 22–73 years, mean 54 ± 14 years) with progressive, histologically proven, unresectable NETs (18 GEP-NETS, one bronchopulmonary neuroendocrine neoplasm, and one renal neuroendocrine carcinoma) were imaged with the SSTR2 antagonist ^{68}Ga-DOTA-JR11 as a prelude to planned therapy with ^{177}Lu-DOTA-JR11 after written informed consent had been provided (trial registration ID NCT02609737). Of these 20 patients, the first six had extended imaging to facilitate kinetic analysis and normal tissue radiation dose estimates.

^{68}Ga-DOTA-JR11 preparation and administration

^{68}Ga-DOTA-JR11 was manufactured by the MSK Radiochemistry and Molecular Imaging Probe Core Facility in compliance with an FDA-approved IND (FDA IND #128,082). The DOTA-JR11 precursor (OctreoPharm, Sciences GmbH, Berlin, Germany) (Supplementary Fig. 1) was labeled with ^{68}Ga using an EZ-102 reagent kit and a 1.85 GBq/50 mCi ^{68}Ga generator supplied by Eckert & Ziegler Radiopharma GmbH, Germany. Briefly, ^{68}Ga was eluted from the generator with ~5 ml of 0.1 N HCl and adsorbed onto an SCX cartridge. The concentrated ^{68}Ga was then eluted from the SCX cartridge using a 5 M NaCl/HCl solution directly into the reactor containing 100 μg of DOTA-JR11 peptide and dissolved in sodium acetate buffer, for a final reaction mixture pH of ~3.7. The reaction mixture was heated to 105 °C for 7 min to allow for radionuclide incorporation. The reaction mixture was then loaded onto a C18 light SEP-PAK cartridge and washed with normal saline to remove unincorporated radionuclide. Finally, ^{68}Ga-DOTA-JR11 was eluted off the purification cartridge with 1 ml of a 1:1 solution of ethanol:water, followed by 9 ml of normal saline, through a 0.22 μm filter, into a sterile, apyrogenic, USP Type I glass vial, sealed with rubber septum and crimped.

The final drug product underwent quality control (QC) testing prior to batch release for patient administration in accordance with acceptance specifications for radiochemical purity, endotoxin content, sterilizing filter integrity, pH, appearance, and radionuclide identity confirmation. Sterility testing was performed post-release.

^{68}Ga-DOTA-JR11 was administered to subjects at a planned activity of 185 MBq (5 mCi) ±10% by slow bolus injection.

Toxicity monitoring

Toxicity monitoring consisted of pre-injection and post-scan vital signs (heart rate, blood pressure, body temperature), pulse oximetry, 3-lead electrocardiography, and monitoring of clinical symptoms.

PET/CT imaging with ^{68}Ga-DOTA-JR11

All 20 patients underwent whole-body (vertex of skull to mid-thigh) PET/CT imaging (GE PET/CT 710 scanner with time-of-flight) at 60 min (mean 64 min; SD 6) post-injection. Patients were asked to void their bladders before imaging. PET scanning was performed in 3-D mode with a 3-min emission time per bed position. A low-dose CT scan (120 kVp, 80 mA tube current, helical pitch 1.5:1; estimated radiation dose 9.0 mGy) was acquired prior to PET imaging for attenuation correction and anatomical localization. Total acquisition time was 18 min or 21 min for six or seven bed positions, respectively. Images were reconstructed using a 700-mm field of view into a 128 × 128 matrix with iterative ordered subset expectation maximization (OSEM: 16 subsets; two iterations) with a 6.4-mm 2D Gaussian post-filter and "heavy" axial 3-point smoothing ([1 2 1]/4). All corrections per manufacturer including CT-based attenuation, scatter, and SharpIR (point spread function correction) were utilized. PET scanner quality assurance as per ACR guidelines, including an ^{18}F well counter calibration, was performed quarterly. Activity quantification for ^{68}Ga PET scans was based on the ^{18}F calibration and knowledge of ratio of positron yields for ^{68}Ga and ^{18}F (i.e., 0.889 to 0.987).

For the purpose of radiation-absorbed dose estimation, additional images were acquired in the first six patients of the 20 accrued (three female and three male). These consisted of a 25-min/19-frame dynamic acquisition initiated at the time of administration and centered on the upper abdomen to include, at least partly, cardiac left ventricle, liver, spleen, and kidney. This was immediately followed at approximately 30 min (mean 34 min; SD 2) post-injection by a whole-body PET/CT scan identical to that acquired at 60 min. Total acquisition time for the dosimetry patient subset was 61–67 min for 6–7 bed positions respectively.

Image interpretation, lesion detection, and data analysis

The whole-body static PET/CT scans acquired at 60 min post-injection were first interpreted without reference to other imaging modalities. Any lesions with focal radiotracer uptake not explained by physiologic SSTR2 expression were interpreted as metastatic disease.

Table 1 Demographic and clinical characteristics of patients

Patient	Sex	Age (years)	Site of primary	Grade
1	F	22	Small intestine	G2
2	F	29	Pancreas	G2
3	M	61	Pancreas	G1
4	M	42	Stomach	G2
5	M	59	BP	atypical
6	F	56	Pancreas	G2
7	M	73	Rectum	G1
8	M	72	Pancreas	G2
9	F	49	Small intestine	G2
10	F	56	Small intestine	G2
11	F	54	Pancreas	G2
12	F	45	Pancreas	G2
13	F	59	Small intestine	G2
14	F	68	Small intestine	G1
15	M	59	Pancreas	G1
16	F	64	Pancreas	G2
17	M	65	Pancreas	G2
18	M	63	Small intestine	G2
19	M	37	Renal	G3
20	M	44	Pancreas	G1

F: female; M: male; BP: bronchopulmonary; G1: low grade (well differentiated); G2: intermediate grade (moderately differentiated); G3: high grade (poorly differentiated)

Volumes of interest (VOI) were generated over lesions using a Hermes imaging workstation (Hermes medical solutions, Chicago, IL, USA). Typically, a value of 40–50% of maximum tracer uptake was used as a threshold, but this was guided by interpretation of the CT scan. A total of 42 lesions were analyzed with a maximum of four lesions per patient.

For normal tissues (liver, kidney, spleen, lung, and cardiac left ventricle), regions of interest (ROI) were drawn within organs over at least five consecutive transaxial PET slices and combined to generate VOIs using a Hermes imaging workstation. For liver, ROI were drawn to exclude, as far as possible, enhanced uptake in disease foci.

Tracer uptake was quantified by standardized uptake values (SUV) normalized to patients' body weight. For lesion VOI, SUV_{max}, and SUV_{peak} were recorded in addition to SUV_{mean}. SUV_{max} referred to the maximum voxel in the VOI, whereas SUV_{peak} was defined as the mean SUV of the hottest 1 cm^3 in the VOI. For normal tissues, only SUV_{mean} within the VOI was used. In the special case of the cardiac left ventricle, the representative value used was the average SUV_{max} over five slices. We have found this quantity to correspond closely to ex-vivo measured blood activity concentration in previous studies.

Comparative lesion uptake was quantified using target-to-normal (TNR) SUV ratios, defined as SUV_{max} (lesion)/SUV

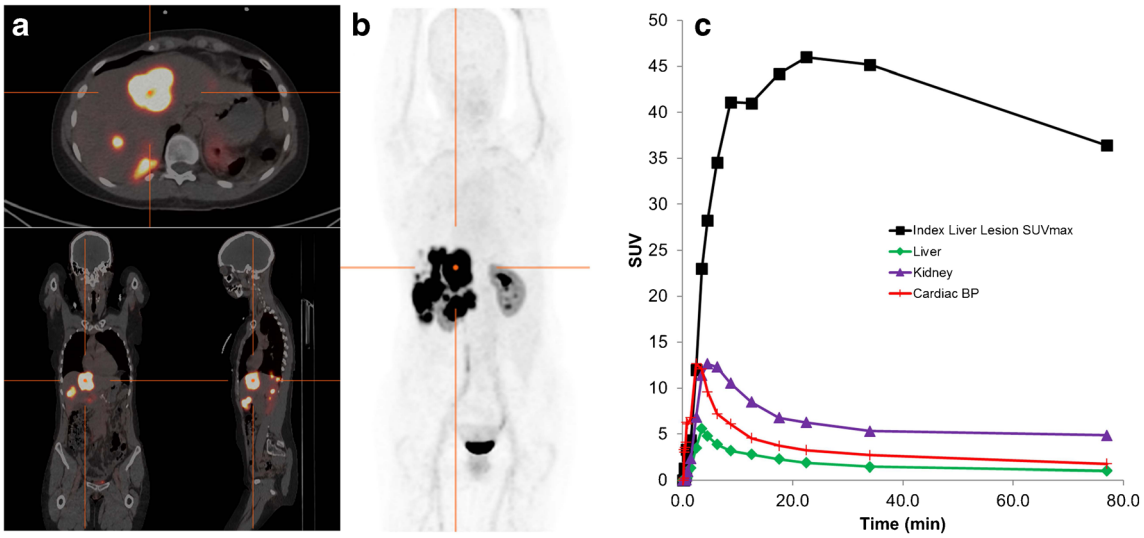

Fig. 1 Patient with predominant liver involvement. **a** Transverse, coronal, sagittal PET/CT image set at the level of the crosshairs shown in **b**. Whole-body maximum-intensity projection images showing the overall distribution of ^{68}Ga-DOTA-JR11. Images acquired at 77 min post-injection demonstrate the lack of significant uptake in any normal tissues, apart from kidney, and show high uptake in hepatic disease. Minimal activity was present in the urinary bladder following pre-scan voiding. **c** SUV-time curves illustrate the rapid uptake of ^{68}Ga-DOTA-JR11 into liver disease with prolonged retention

(tissue) for blood, spleen, kidney, and liver. As four of the 20 patients had prior splenectomy, TNR (spleen) was calculated for only 16 patients.

Absorbed dose calculations

Absorbed radiation doses to normal tissues were estimated in a subset of six patients who had additional imaging as described above. Absorbed doses to whole body (WB) and individual organs were calculated based on the combined dynamic and static PET/CT images. Activity concentration–time curves for all organs displaying ^{68}Ga-DOTA-JR11 accumulation were generated by VOI analysis. For liver, this curve was for normal (uninvolved) liver. It was assumed that the red marrow activity concentration was equal to that of blood [10]. WB activity-time curves were generated using the three points defined by the administered activity (time zero) and the total activities in the two whole-body PET scans. These data

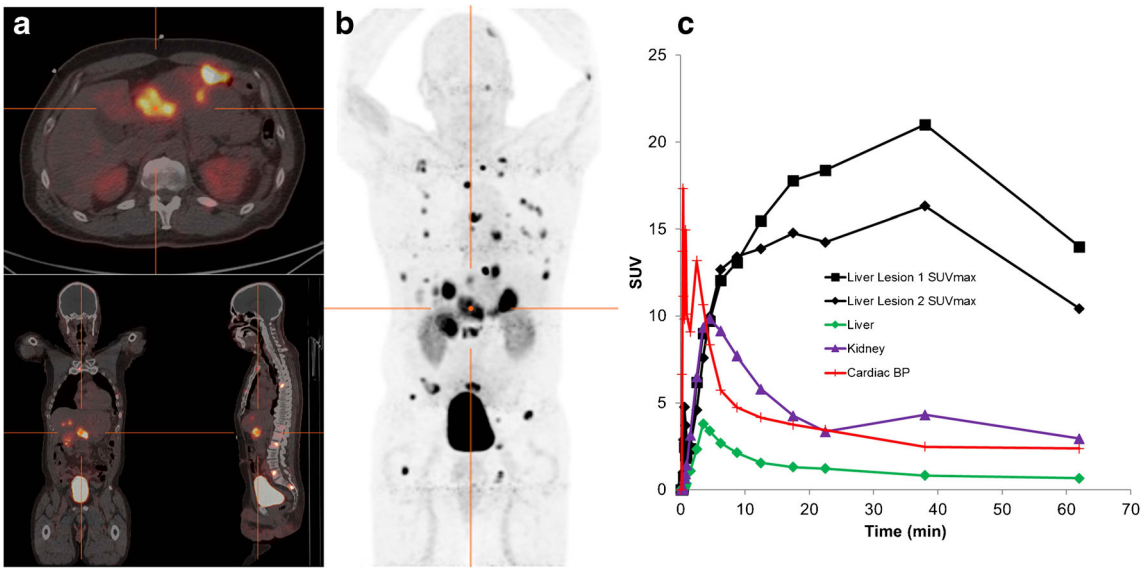

Fig. 2 Patient with atypical broncho-pulmonary NET with hepatic and osseous metastases. **a** Transverse, coronal, sagittal PET/CT image set at the level of the crosshairs shown in **b**. Whole-body maximum-intensity projection images showing overall ^{68}Ga-DOTA-JR11 distribution. Images acquired at 62 min post-injection demonstrate the lack of significant normal tissue uptake, apart from kidney. Focal uptake is seen in hepatic and osseous metastases. There is significant activity (approximately 15% of the administered amount) in the urinary bladder, illustrating the primary route of excretion. **c** SUV-time curves show rapid uptake of ^{68}Ga-DOTA-JR11 into lesions

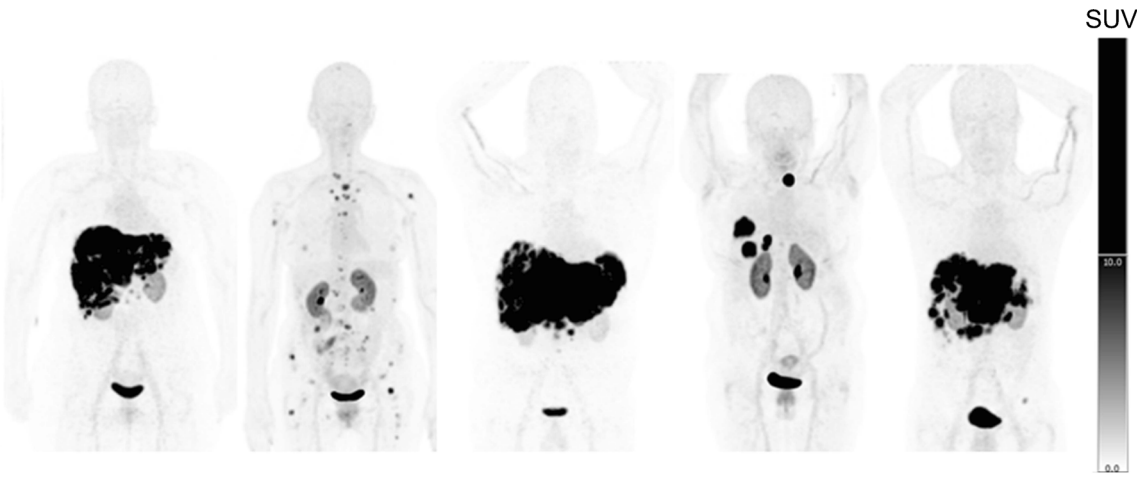

Fig. 3 Panel of five whole-body maximum-intensity projection images acquired at 60 min post-injection, demonstrating intense focal uptake in metastases and minimal background uptake, resulting in excellent image contrast

were used to calculate mono-exponential biological half-times for WB clearance.

The areas under activity concentration–time curves (AUC) were estimated by trapezoidal integration of the combined data from dynamic and static images with a terminal contribution calculated by extrapolation from the last measured value, using the shorter of apparent terminal clearance rate or physical decay. Whole-organ AUCs were estimated by multiplying the activity concentration AUC by organ mass, as taken from the OLINDA/EXM 1.0 software application [11]. We did not use patient mass-based rescaling in this study, as the actual patients' masses did not differ substantially from OLINDA/EXM 1.0 standard values (73.7 kg for male; 56.9 kg for female). The number of disintegrations in normal organs (i.e., residence times) were derived by dividing whole-organ AUC by the administered activity. For urinary bladder contents, residence times were derived using the voiding bladder model built into OLINDA/EXM 1.0, the estimated mono-exponential whole-body biological half-time, and an assumed voiding interval of 1 h. This relatively short time was deemed appropriate for this short-lived radiopharmaceutical, considering that patients were instructed to void their bladders before the 60-min PET scan and encouraged to hydrate and void frequently thereafter. Residence times for the remainder of body were derived by subtracting all the individually estimated residence times from the whole-body residence time. Absorbed radiation doses to the whole body and various organs were calculated using the OLINDA/EXM 1.0 software application [11]. Subsequently, effective doses were recalculated using the tissue weighting factors promulgated in ICRP Report 103 [12].

Table 2 SUV_{mean} of organs for the 60-min whole-body scan (normal liver, spleen, kidney)

Organ	SUV_{mean}
Liver ($n = 19$)	1.1 ± 0.3
Spleen ($n = 16$)	1.4 ± 0.3
Kidney ($n = 20$)	4.5 ± 1.5

Data are mean ± SD

Results

^{68}Ga-DOTA-JR11 administration and safety

Patient characteristics are summarized in Table 1. All 20 enrolled patients were administered ^{68}Ga-DOTA-JR11, underwent at least one whole-body PET/CT, and are included in the analysis. The mean administered activity was 169 MBq (4.6 mCi); range: 137–192 MBq (3.7-5.2 mCi) with a mean radiochemical purity of 99.95% (range: 99–100%). The mean injected peptide mass was 81 μg (range: 60–97 μg) (Supplementary Table 1).

Of the 20 patients, 18 experienced no infusion-related symptoms. Two patients with hormone-secreting tumors experienced flushing (G3/2), hypotension (G3/G1), and nausea (G1). Of these, one experienced additional tachycardia (G1), abdominal pain (G2), and diarrhea (G1), requiring injection of 150 μg Octreotide s.c. No significant changes (pre- vs. post-injection) were evident in blood glucose, body temperature, peripheral oxygen saturation, or EKG. No subsequent adverse events were observed in the follow-up period (mean 16 days; range 2–30 days) prior to PRRT.

PET/CT imaging with ^{68}Ga-DOTA-JR11

^{68}Ga-DOTA-JR11 PET/CT revealed positive lesions in all 20 patients. On visual inspection, images demonstrated favorable biodistribution with little or no uptake in the pituitary, parotid, and salivary glands, thyroid, spleen, adrenals, and uninvolved liver (Figs. 1, 2, and 3). Quantitative analysis indicated little uptake above blood pool in organs such as spleen (SUV_{mean}

Table 3 SUV and TNR for 42 reference lesions at 60 min post-administration

Site	*N*	SUV_{max}	SUV_{mean}	SUV_{peak}	TNR-B	TNR-S	TNR-K	TNR-L
Lung	1	17	7.4	11	11	9	2.3	15
Liver	30	25 ± 22	11 ± 9	21 ± 19	22 ± 20	12 ± 12	6 ± 6	23 ± 23
LN	8	14 ± 20	7 ± 6	12 ± 19	10 ± 14	4 ± 3	2.3 ± 3.1	12 ± 17
Bone	3	6 ± 3	4 ± 2	5 ± 2	5 ± 3	4 ± 2	1.4 ± 0.3	6 ± 1
Total	42	21 ± 21	10 ± 8	18 ± 19	18 ± 19	10 ± 11	5 ± 6	20 ± 21

TNR: tumor-to-normal tissue (SUV_{max}/SUV_{mean}) ratio; B: blood; S: spleen; K: kidney; L: normal liver. Data are mean ± SD

1.4; range 0.7–1.8; $n = 16$) and uninvolved liver (SUV_{mean} 1.1; range 0.7–1.9; $n = 19$). Renal uptake was higher with an SUV_{mean} of 4.5; range 1.3–7.2 (Table 2). The main route of excretion was renal, and substantial urinary bladder activity was observed in patients who had whole-body PET/CT images at 30 min post-administration, amounting to a median of 15% of the administered activity (range 12–26%; $n = 6$). However, in most cases, this was significantly reduced at the time of the 60-min image before which patients were instructed to void.

A total of 42 lesions were examined on whole-body ^{68}Ga-DOTA-JR11 PET/CT ($n = 4$, 3 pts.; $n = 3$, 3 pts.; $n = 2$, 7 pts.; $n = 1$, 7 pts). Liver was the most common site of disease with 30 lesions, followed by lymph nodes ($n = 8$), bone ($n = 3$), and lung ($n = 1$). Lesion uptake at 60 min was variable with median SUV_{max} of 13 (range: 2.9–94) and SUV_{peak} of 10 (2.5–84) (see also Table 3). There were a wide range of tumor sizes ranging from a small vertebral lesion (1.4 ml) up to a very large lesion that encompassed almost the entire liver (1100 ml) with a median lesion volume of 15 ml. Although partial volume averaging effects inevitably lead to an underestimate of lesion uptake at small sizes, there was no statistically significant trend between lesion volume and SUV_{max} ($r^2 = 0.16$). A full list of lesion volumes and associated SUV_{max} is provided in Supplementary Table 2.

In the six patients who had dynamic images, lesion uptake was observed to be rapid (Figs. 1 and 2), typically reaching the highest levels (SUV_{max} of up to 50) by 20–30 min post-injection and in most instances remaining close to plateau thereafter. Blood clearance was generally rapid, but with a low-level terminal component that cleared more slowly, corresponding to a median time-zero SUV intercept of 3.7 clearing with a median biological halftime of 60 min.

Absorbed dose estimates for ^{68}Ga-DOTA-JR11

Normal tissue residence times for six patients are provided in Table 4. Those for red marrow and cardiac contents were generated from the blood activity–time curves. The full set of normal tissue absorbed dose estimates (mGy/MBq) are shown in Table 5. The highest values were (mean ± SD): urinary bladder wall (0.30 ± 0.06), kidneys (0.050 ± 0.013), liver (0.023 ± 0.014), lungs (0.021 ± 0.05), heart wall (0.020 ± 0.04), and spleen (0.018 ± 0.002). The estimated effective dose (ICRP 103) was 0.022 ± 0.003 mSv/MBq.

Discussion

This first-in-human study of ^{68}Ga-DOTA-JR11 demonstrated very favorable biodistribution, with only minimal tracer uptake in normal parenchymal organs except for the kidneys. Tumor uptake was rapid, and resulted in high-contrast images of metastatic NETs. In particular, the low background activity in liver was advantageous and facilitated detection of liver metastases. These characteristics make ^{68}Ga-DOTA-JR11 an attractive companion diagnostic for patient selection for therapy with ^{177}Lu-DOTA-JR11.

The reasons for differences in normal tissue uptake of ^{68}Ga-DOTA-JR11 and the known biodistribution of

Table 4 Residence times (hours) in selected organs ($n = 6$)

Patient	Kidney	Liver	Spleen	Lung	RM	C Cont	UB	RoB	WB
1	0.028	0.049	0.0050	0.024	0.053	0.015	0.24	0.40	0.82
2	0.017	0.032	0.0058	0.027	0.070	0.032	0.20	0.57	0.95
3	0.040	0.050	N/A	0.045	0.088	0.025	0.22	0.42	0.88
4	0.027	0.133	0.0041	0.031	0.067	0.019	0.18	0.53	1.00
5	0.030	0.048	0.0071	0.040	0.056	0.025	0.26	0.31	0.77
6	0.033	0.079	0.0071	0.053	0.078	0.035	0.20	0.45	0.93

RM: red marrow; C Cont: cardiac contents; UB: urinary bladder; RoB: remainder of body; WB: whole body; N/A: not available

Table 5 Absorbed doses to normal tissues from ^{68}Ga-DOTA-JR11 (n = 6)

Target organ	Patient						
	1	2	3	4	5	6	Mean ± SD
Adrenals	0.007	0.007	0.008	0.009	0.005	0.007	0.007 ± 0.002
Brain	0.004	0.005	0.005	0.006	0.003	0.004	0.004 ± 0.001
Breasts	0.005	0.005	0.005	0.006	0.003	0.004	0.005 ± 0.001
GB wall	0.007	0.007	0.007	0.010	0.005	0.007	0.007 ± 0.002
LLI wall	0.009	0.008	0.009	0.010	0.007	0.007	0.008 ± 0.001
Small intestine	0.007	0.007	0.007	0.008	0.005	0.006	0.007 ± 0.001
Stomach wall	0.006	0.006	0.006	0.008	0.004	0.005	0.006 ± 0.001
ULI wall	0.007	0.007	0.007	0.009	0.004	0.006	0.007 ± 0.001
Heart wall	0.014	0.023	0.021	0.019	0.017	0.024	0.020 ± 0.004
Kidneys	0.049	0.029	0.070	0.048	0.048	0.053	0.050 ± 0.013
Liver	0.020	0.010	0.020	0.050	0.015	0.023	0.023 ± 0.014
Lungs	0.016	0.015	0.027	0.021	0.020	0.026	0.021 ± 0.005
Muscle	0.006	0.006	0.006	0.007	0.004	0.005	0.006 ± 0.001
Ovaries	0.009	N/A	0.009	0.010	N/A	N/A	0.009 ± 0.000
Pancreas	0.006	0.007	0.007	0.009	0.005	0.006	0.007 ± 0.001
Red marrow	0.013	0.017	0.019	0.017	0.013	0.018	0.016 ± 0.003
Osteogenic cells	0.015	0.015	0.021	0.020	0.011	0.015	0.016 ± 0.004
Skin	0.004	0.005	0.005	0.006	0.003	0.004	0.004 ± 0.001
Spleen	0.018	0.017	N/A	0.016	0.020	0.020	0.018 ± 0.002
Testes	N/A	0.007	N/A	N/A	0.005	0.006	0.006 ± 0.001
Thymus	0.005	0.006	0.006	0.007	0.004	0.005	0.006 ± 0.001
Thyroid	0.005	0.005	0.005	0.006	0.003	0.004	0.005 ± 0.001
UB wall	0.378	0.230	0.343	0.289	0.297	0.237	0.30 ± 0.06
Uterus	0.013	N/A	0.013	0.013	N/A	N/A	0.013 ± 0.000
Total body	0.007	0.007	0.008	0.010	0.005	0.007	0.007 ± 0.001
Effective dose (mSv/MBq)	0.024	0.018	0.025	0.023	0.020	0.020	0.022 ± 0.003

GB: gall bladder; LLI: lower large intestine; ULI: upper large intestine; UB: urinary bladder

Effective doses were calculated using ICRP 103 weighting factors

Data are in mGy/MBq unless otherwise specified

somatostatin receptor antagonists are currently not well understood. Specifically, the lack of uptake by organs with known SSTR2 expression, such as the adrenals and the pituitary gland, is intriguing and requires further study. Contributory

Table 6 Absorbed doses in selected organs using selected SSTR2 tracers

Target organ	^{68}Ga-DOTA-JR11	^{68}Ga-DOTA-TATE [3]	^{68}Ga-DOTA-TATE [14]	^{68}Ga-DOTA-TOC [14]	^{68}Ga-NODAGA-JR11 [8]
Kidney	0.050 ± 0.013	0.092 ± 0.028	0.093 ± 0.016	0.082 ± 0.020	0.084 ± 0.031
Liver	0.023 ± 0.014	0.045 ± 0.015	0.050 ± 0.015	0.041 ± 0.014	0.022 ± 0.009
Spleen	0.018 ± 0.002	0.28 ± 0.12	0.109 ± 0.058	0.108 ± 0.065	0.06 ± 0.05
Adrenals	0.007 ± 0.002	0.015 ± 0.001	0.086 ± 0.052	0.077 ± 0.028	0.03 ± 0.01
Lungs	0.021 ± 0.005	0.012 ± 0.0004	0.006 ± 0.001	0.007 ± 0.001	0.021 ± 0.007
UB wall	0.30 ± 0.06	0.12 ± 0.06	0.098 ± 0.048	0.12 ± 0.058	0.10 ± 0.04
Red marrow	0.016 ± 0.003	0.010 ± 0.0003	0.015 ± 0.003	0.016 ± 0.003	0.011 ± 0.003
Total body	0.007 ± 0.001	0.014 ± 0.0003	0.014 ± 0.002	0.014 ± 0.002	N/A
Effective dose (mSv/MBq)	0.022 ± 0.003	0.026 ± 0.003	0.021 ± 0.003	0.021 ± 0.003	0.024 ± 0.002

Mean ± SD are provided. Data are absorbed dose in mGy/MBq unless otherwise specified

factors may include the SSTR2 antagonistic properties of ^{68}Ga-DOTA-JR11, the possibility of large disease "sinks" reducing agent availability, and the higher peptide mass administered. It should be noted, however, that adrenal/pituitary uptake was not seen, even for patients with low disease burdens, while the rationale for using a higher peptide mass was for compatibility with subsequent PRRT using ^{177}Lu-DOTA-JR11, which all patients went on to have.

In a recent preclinical study, Nicolas et al. evaluated the effect of peptide mass on the biodistribution and dosimetry of ^{177}Lu-DOTA-JR11 [13]. Escalating amounts (10, 200, and 2000 pmol) did not lead to saturation of binding sites on tumor, but greatly suppressed uptake in normal SSTR2-expressing organs, thereby increasing tumor-to-background ratios.

Irrespective of its cause, the low uptake by most normal parenchymal organs resulted in favorable radiation dosimetry for ^{68}Ga-DOTA-JR11 when compared with published data on Gallium-labeled somatostatin receptor agonists. For example, liver and kidney doses were up to 50% lower than those reported for ^{68}Ga-DOTA-TOC or ^{68}Ga-DOTA-TATE [3, 14], while spleen dose was less by a factor of 6-15 (Table 6). Here, it should be noted that the existence of large disease sinks, especially in the liver, could lead to an underestimate of absorbed dose to normal liver, kidney, and spleen, as any contribution due to photon irradiation from liver disease-associated activity was not considered. The impact of this effect will vary from patient to patient, depending on the amount and biodistribution of disease, and will be alleviated to some extent by the inclusion of the cross-dose contribution from activity in the remainder-of-body compartment.

Because of large variabilities in tumor uptake of SSTR2-targeting imaging agents, it is not straightforward to objectively compare ^{68}Ga-DOTA-JR11 with somatostatin receptor agonists. However, the high image contrast observed in this study with SUVmax up to 94 is certainly comparable to SUVmax reported for somatostatin receptor agonists.

Nicolas et al. [8, 9] recently reported the clinical use of ^{68}Ga-NODAGA-JR11 (^{68}Ga-OPS202) to image GEP-NETs. The use of ^{68}Ga-NODAGA-JR11 is supported by preclinical studies [7], which indicated that labeling DOTA-JR11 with ^{68}Ga reduced its SSTR2 binding affinity by a factor of approximately 80, whereas labeling NODAGA-JR11 with ^{68}Ga had no impact on SSTR2 binding. Interestingly, our data indicate that despite the lower affinity of ^{68}Ga-DOTA-JR11, substantial tumor uptake and high-contrast images are feasible. Our findings suggest that, in the range studied, receptor binding affinity may not be the key factor determining in-vivo tumor uptake. The normal tissue distributions of ^{68}Ga-DOTA-JR11 and ^{68}Ga-NODAGA-JR11 were broadly similar, with somewhat higher uptake of ^{68}Ga-NODAGA-JR11 by kidney and around three times higher for the spleen, resulting in higher radiation doses for these organs. Additionally, despite its lower affinity, ^{68}Ga-DOTA-JR11 at a peptide mass dose of 80 μg (±10) had somewhat higher uptake in liver metastases (median SUV_{max} 18) than ^{68}Ga-NODAGA-JR11 (median SUV_{max} 10.9, 12.6 at peptide mass doses of 15 and 50 μg), and was broadly similar for all lesions combined (median SUV_{max} 13 for ^{68}Ga-DOTA-JR11 vs 12.3, 14.4 for ^{68}Ga-NODAGA-JR11 at 15 and 50 μg).

^{68}Ga-DOTA-JR11 administration was well tolerated in 18 out of 20 patients. However, two patients with functional NETs experienced symptoms with flushing, grade 3 hypotension, nausea, and lightheadedness, possibly related to the SSTR2 antagonistic properties of ^{68}Ga-DOTA-JR11. To our knowledge, this is in contrast to studies evaluating the safety of ^{68}Ga-labeled agonists such as DOTA-TATE [3], which did not report any physiologic responses to the radiopharmaceutical. Therefore, administration of ^{68}Ga-DOTA-JR11 by infusion may be preferable to slow bolus injection.

Conclusion

^{68}Ga-DOTA-JR11 is a promising companion diagnostic for selection of patients for therapy with ^{177}Lu-DOTA-JR11. The unexpected yet favorable biodistribution of ^{68}Ga-DOTA-JR11 requires further studies to better understand the impact of peptide mass, disease burden, and SSTR2 antagonistic properties of ^{68}Ga-DOTA-JR11. Because of the large variability of SSTR2 expression in NETs, head-to-head comparisons in specific patient groups would probably be required to determine whether ^{68}Ga-DOTA-JR11 or ^{68}Ga-NODAGA-JR11 are preferable for detection and staging of NETs.

Acknowledgements This study was supported in part by the Geoffrey Beene Cancer Research Center at MSK and the MSK Radiochemistry and Molecular Imaging Probe Core, which is funded in part through the NIH/NCI Cancer Center Support Grant P30 CA008748. We gratefully acknowledge funding by Caring for the Carcinoid/NETRF. SK was supported in part by the NIH/NCI Paul Calabresi Career Development Award for Clinical Oncology K12 CA184746. The precursor used in this study was provided by Ipsen.

We gratefully acknowledge Rashid Ghani and members of the Nuclear Medicine Pharmacy; nuclear medicine nurses Ann Longing and Louise Harris for their help in patient management; RSAs Alicia Lashley, Hanh Pham, and Martha Ziolkowska and Clinical Research Manager Bolorsukh Gansukh for their excellent support with patient flow and protocol management; the radiation safety officers and nuclear medicine technologists for their excellent technical assistance; and members of the Department of Medicine at MSK for patient referral. We also thank Leah Bassity for her assistance in editing this manuscript.

Funding This study was supported in part by the Geoffrey Beene Cancer Research Center at MSK, and the MSK Radiochemistry and Molecular Imaging Probe Core was funded in part through the NIH/NCI Cancer Center Support Grant P30 CA008748. We gratefully acknowledge the funding by Caring for the Carcinoid/NETRF. SK was supported in part by NIH/NCI Paul Calabresi Career Development Award for Clinical Oncology K12 CA184746. The precursor used in this study was provided by Ipsen.

Compliance with ethical standards

Conflict of interest DR was a member of the Advisory Board for Ipsen, Novartis, Advanced Accelerator Applications (AAA), and Lexicon Pharmaceuticals and has received research funding from Ipsen and Novartis. LB acted as a consultant for Advanced Accelerator Applications (AAA) and Ipsen. WW has served as a consultant for Endocyte, Ipsen, and Piramal Imaging. JAD has served as a consultant to WILEX AG, Algeta ASA, and Janssen Pharmaceuticals, Inc. SK, NP, BJB, SKL, and JSL declare that they have no conflict of interest.

Ethical approval All procedures performed in studies involving human participants were in accordance with the ethical standards of the institutional and/or national research committee and with the1964 Helsinki Declaration and its later amendments or comparable ethical standards.

Informed consent Informed written consent was obtained from all individual participants included in the study.

References

1. Lawrence B, Gustafsson BI, Chan A, Svejda B, Kidd M, Modlin IM. The epidemiology of gastroenteropancreatic neuroendocrine tumors. Endocrinol Metab Clin N Am. 2011;40:1–18 vii.
2. Kaltsas GA, Mukherjee JJ, Grossman AB. The value of radiolabelled MIBG and octreotide in the diagnosis and management of neuroendocrine tumours. Ann Oncol. 2001;12(Suppl 2): S47–50.
3. Walker RC, Smith GT, Liu E, Moore B, Clanton J, Stabin M. Measured human dosimetry of 68Ga-DOTATATE. J Nucl Med. 2013;54:855–60.
4. Ginj M, Zhang H, Waser B, Cescato R, Wild D, Wang X, et al. Radiolabeled somatostatin receptor antagonists are preferable to agonists for in vivo peptide receptor targeting of tumors. Proc Natl Acad Sci U S A. 2006;103:16436–41.
5. Cescato R, Waser B, Fani M, Reubi JC. Evaluation of 177Lu-DOTA-sst2 antagonist versus 177Lu-DOTA-sst2 agonist binding in human cancers in vitro. J Nucl Med. 2011;52:1886–90.
6. Wild D, Fani M, Fischer R, Del Pozzo L, Kaul F, Krebs S, et al. Comparison of somatostatin receptor agonist and antagonist for peptide receptor radionuclide therapy: a pilot study. J Nucl Med. 2014;55:1248–52.
7. Fani M, Braun F, Waser B, Beetschen K, Cescato R, Erchegyi J, et al. Unexpected sensitivity of sst2 antagonists to N-terminal radiometal modifications. J Nucl Med. 2012;53:1481–9.
8. Nicolas GP, Beykan S, Bouterfa H, Kaufmann J, Bauman A, Lassmann M, et al. Safety, biodistribution, and radiation dosimetry of (68)Ga-OPS202 ((68)Ga-NODAGA-JR11) in patients with gastroenteropancreatic neuroendocrine tumors: a prospective phase I imaging study. J Nucl Med. 2017;59(6):909–14.
9. Nicolas GP, Schreiter N, Kaul F, Uiters J, Bouterfa H, Kaufmann J, et al. Sensitivity comparison of (68)Ga-OPS202 and (68)Ga-DOTATOC PET/CT in patients with gastroenteropancreatic neuroendocrine tumors: a prospective phase II imaging study. J Nucl Med. 2018;59:915–21.
10. Forrer F, Krenning EP, Kooij PP, Bernard BF, Konijnenberg M, Bakker WH, et al. Bone marrow dosimetry in peptide receptor radionuclide therapy with [177Lu-DOTA(0),Tyr(3)]octreotate. Eur J Nucl Med Mol Imaging. 2009;36:1138–46.
11. Stabin MG, Sparks RB, Crowe E. OLINDA/EXM: the second-generation personal computer software for internal dose assessment in nuclear medicine. J Nucl Med. 2005;46:1023–7.
12. IRCP. The 2007 Recommendations of the International Commission on Radiological Protection. ICRP publication 103. Ann ICRP. 2007;37:1–332.
13. Nicolas GP, Mansi R, McDougall L, Kaufmann J, Bouterfa H, Wild D, et al. Biodistribution, pharmacokinetics, and dosimetry of (177)Lu-, (90)Y-, and (111)in-labeled somatostatin receptor antagonist OPS201 in comparison to the agonist (177)Lu-DOTATATE: the mass effect. J Nucl Med. 2017;58:1435–41.
14. Sandstrom M, Velikyan I, Garske-Roman U, Sorensen J, Eriksson B, Granberg D, et al. Comparative biodistribution and radiation dosimetry of 68Ga-DOTATOC and 68Ga-DOTATATE in patients with neuroendocrine tumors. J Nucl Med. 2013;54:1755–9.